Oscillatory Shear Rheology of Dilute Solutions of Flexible Polymers Interacting with Oppositely Charged Particles

Rangarajan Radhakrishnan and Patrick T. Underhill
Dept. of Chemical and Biological Engineering, Rensselaer Polytechnic Institute, Troy, NY 12180

DOI 10.1002/aic.14380
Published online February 6, 2014 in Wiley Online Library (wileyonlinelibrary.com)

Fluids with both attractions and repulsions among its constituents can exist in multiple states depending on nature of the interactions. An external flow can induce such systems to transition between the different states, such as the globule-stretch transition for polymers in poor solvents. Brownian dynamics simulations of a dilute solution of polymers and colloids interacting via short-ranged potentials are presented. For some values of the strength and range of interactions, compact structures of polymers and colloids are formed. An external flow is capable of pulling these globules apart, causing the polymers to stretch at a critical shear rate. In oscillatory shear, the shear rate can cycle between being above and below this critical shear rate leading to interesting dynamics. These dynamics are quantified using the rheological response in large amplitude oscillatory shear. © 2014 American Institute of Chemical Engineers *AIChE J*, 60: 1365–1371, 2014

Keywords: complex fluids, rheology, polymer properties

Introduction

In a number of different polymeric systems, changing the attractive and repulsive interactions between their components can change the optical, mechanical, electrical, and rheological properties.[1–3] The changes in their properties are due to the different states that these systems can exist in. Many of these systems, even in dilute solutions, show formation of compact structures in flow or in equilibrium. Examples of such systems include polymers in poor solvents,[4,5] polyelectrolytes,[6–8] mixtures of polymers and colloids,[9,10] and others[11,12] Interactions between the polymer segments of a long polymer can be mediated by salt ions, nanoparticles,[2,9,10,13,14] surfactant micelles,[15–17] proteins,[18–20] and other small molecules.[21–23] Changing the conditions such as temperature, salt concentration, and pH changes the interactions and thereby the material properties.

Theoretical understanding of such systems can be aided by modeling and simulation studies. However, large differences in the time and length scales of interactions and relaxation of long polymers makes detailed atomic simulations expensive. Simple coarse-grained models have been used to facilitate study of such systems. A polymer is usually modeled as a chain of beads connected by "entropic" springs. The interactions between different segments of the polymer are captured using effective interactions between beads of the model. Using such a model, Alexander-Katz and coworkers[24–27] have studied the globule formation and break up of self-associating polymers. Hoda and Larson[28] used a model of hydrophobic polyelectrolytes with bead–bead attractions and spring–spring repulsions and found that shear induces cluster formation. We examine here a mixture of a polymer and nanoparticles in which there are short-ranged attractions between the two. A nanoparticle can bridge polymer segments, leading to an effective attraction between them. We have recently used a coarse-grained model of this type of mixture in steady shear flow to examine the formation of compact globule structures and a globule-stretch transition (Radhakrishnan and Underhill, under review).

Oscillatory flows have been extensively to probe the properties of fluids. Recently, large amplitude oscillatory shear (LAOS) has been used by many researchers to probe both the time-dependent and nonlinear properties of materials (see, e.g., review in Ref. 29). In oscillatory flow the shear rate, quantified by the Weissenberg number Wi, and frequency, quantified by the Deborah number De, can be independently varied. Both are expected to have an important role here with a system that undergoes a globule-stretch transition. If Wi is below a critical value, the system will stay in globules for all De. At larger Wi, the De will be important in determining the response because of the two states the system can exist in. Both the globules and stretch states have a characteristic relaxation time that will determine the response of each state, but there is also a characteristic timescale for the system to transition between states. The interplay of these three timescales and their comparison the imposed frequency of oscillation will lead to LAOS response not typical for polymeric materials. There are efforts to use the LAOS response as a way to categorize materials,[30] and the response seen here may be characteristic of many systems that can exist in multiple states. Another example of polymers undergoing a transition between states is the coil-stretch transition in steady elongational flow.[31–33] Future work could examine whether oscillatory elongational flows

Correspondence concerning this article should be addressed to P. T. Underhill at underhill@rpi.edu.

show similarly features to the oscillatory shear flows examined here.

Model Description and Simulation Methodology

In this article, a coarse-grained model of a polymer interacting with colloids developed by Radhakrishnan and Underhill (under review) is used. At a coarse level, a flexible polymer can be modeled as a freely jointed chain made of N_K number of very stiff rods of length l called the Kuhn length. At an even coarser level, this freely jointed chain can be represented as a bead-spring chain in which the springs represent the entropic cost of stretching the polymer. A common approximation is to use finitely extensible nonlinear elastic (FENE) springs,[34] whose force is given as

$$F_{\mathrm{FENE}}(Q)=\frac{3k_BTQ}{R_H^2(1-(Q/Q_0)^2)} \tag{1}$$

where Q is extension of a spring, k_{B} is Boltzmann's constant, T is the absolute temperature, $R_H^2=N_{K,s}l^2, N_{K,s}$ are number of Kuhn steps represented by a spring, and $Q_0=N_{K,s}l$ is the maximum length of the spring. The length R_H is an approximation of the root-mean-squared length of a spring at equilibrium that is accurate if the spring is approximately Hookean (if Q_0 is very large). The beads of the model represent the points along the polymer where forces act. The nanoparticles in solution are modeled as spheres. To have attractions between the polymer and nanoparticles, we consider them both to be charged with opposite signs and that there is enough dissolved salt in solution to screen-out much of the attractions. The Debye–Huckel (DH) potential approximates this interaction in which the solvent and dissolved salt is treated implicitly and is given by

$$U_{\mathrm{DH}}(r_{ij})=\frac{A^*k_BTR_H}{r_{ij}}\exp\left(-\kappa^*\frac{r_{ij}}{R_H}\right) \tag{2}$$

where

$$A^*=\frac{1}{k_BTR_H}\frac{q_iq_j}{4\pi\epsilon_0\epsilon_r} \tag{3}$$

quantifies the strength of interaction between beads i and j with charges q_i and q_j in a material with dielectric constant ϵ_r, permittivity of vacuum ϵ_0, and separation between the beads r_{ij}. The parameter $\kappa^*=\kappa R_H$ determines the range of interaction, where κ^{-1} is the Debye length. To prevent overlap of a polymer bead and a nanoparticle bead, a repulsive Weeks–Chandler–Andersen potential[35] is used and is given by

$$U_{\mathrm{WCA}}(r_{ij})=\begin{cases}4\epsilon\left[\left(\frac{\sigma}{r_{ij}}\right)^{12}-\left(\frac{\sigma}{r_{ij}}\right)^{6}\right]+\epsilon & r_{ij}<2^{1/6}\sigma\\ 0 & r_{ij}\geq 2^{1/6}\sigma\end{cases} \tag{4}$$

where ϵ determines the strength of interaction and σ is the range of interaction. In another article (Radhakrishnan and Underhill, under review), we have shown that a simulation system consistent with some experimental systems uses a polymer bead-spring chain with $N=10$ beads, $N_{k,s}=9$ number of Kuhn steps per spring, $\epsilon=k_BT/12$, and $\sigma=0.1R_H$. Periodic boundary conditions are used on the simulation domain, which contains a single polymer and $N_{\mathrm{col}}=200$ nanoparticles. One polymer is used to focus on the dilute limit without interactions between polymers. The simulation domain was chosen large enough that the results only depend on the concentration of nanoparticles (and not the exact number). This nanoparticle concentration is dilute and in part determines whether it is favorable for them to condense onto the polymer backbone.

For simplicity, we take the charge on a polymer bead and nanoparticle bead to be equal in magnitude, and will quantify the electrostatic interactions using a positive value of A^*. This represents the repulsion between like charges, while the attractions are of the same magnitude. Equilibrium simulations and an equilibrium model (Radhakrishnan and Underhill, under review) show that A^* and κ^* ranging from 1 to 10 is the useful regime to examine. In particular, for weak attraction part of this range, the polymers remain in the coiled state at equilibrium, whereas for larger attractions the polymer and nanoparticles condense into a compact globule structure that can undergo a globule-stretch transition in flow. All simulations in this article use $\kappa^*=10$, which corresponds to a Debye length approximately equal to the Kuhn length of the polymer. This is a common experimental condition for flexible polymers until high salt conditions. The parameter A^* alters the binding energy between the polymer and colloid beads, which is in the range of 1–10 times k_BT here.

The motion of the polymer and colloid beads is computed by means of Brownian dynamics (BD) simulation methodology. BD has been widely used to study the properties of polymers and colloids.[36–47] In this methodology, the beads obey Newton's laws of motion in an implicit solvent and a stochastic term accounts for the thermal fluctuations. In accordance with Newton's laws of motion, the balance of forces acting on any bead is given by

$$m\ddot{\mathbf{r}}=\mathbf{F_s}+\mathbf{F_d}+\mathbf{F_B} \tag{5}$$

where $\mathbf{F_B}$ is the Brownian force, $\mathbf{F_s}$ are the systematic forces (which includes external and spring forces), and $\mathbf{F_d}$ is the drag force. The acceleration term can be neglected if the mass of the particle is very small ($m\rightarrow 0$) and only the balance of other forces are considered

$$\mathbf{F_s}+\mathbf{F_d}+\mathbf{F_B}\approxeq 0 \tag{6}$$

The above equation corresponds to tracking the motion of the particle at time scales larger than the inertia or momentum relaxation time scale.

Neglecting hydrodynamic interactions, the drag force on a bead at a distance $\mathbf{r}$ from the origin at very low Reynolds number is given by

$$\mathbf{F_d}=-\zeta\left(\mathbf{v_p}-\mathbf{v_s}(\mathbf{r})\right) \tag{7}$$

where ζ is the drag coefficient of the bead, $\mathbf{v_p}=\dot{\mathbf{r}}$ is the velocity of the particle, and $\mathbf{v_s}(\mathbf{r})$ is the velocity of the undisturbed solvent at that bead's position. For simplicity, the drag coefficient of a bead in the polymer bead-spring chain and for a nanoparticle is assumed to be the same. This is also done because the average length of a spring equals the size of a colloid. The random Brownian force $\mathbf{F_B}$ is taken such that $\langle\mathbf{F_B}(t)\cdot\mathbf{F_B}(s)\rangle=2K_BT\zeta\delta(t-s)$ and $\langle\mathbf{F_B}\rangle=0$ to satisfy the fluctuation dissipation theorem.[38] Hydrodynamic interactions can change the details of the globule-stretch transition and the relaxation spectrum of a stretched polymer. Therefore, it is expected that the quantitative details of our simulations would change slightly if these interactions were

included. However, because they are not needed to consider the phenomena shown here, they are not included. In this way, we are trying to examine the simplest system that shows the phenomena to better understand the necessary features.

The simulations are performed in an externally imposed oscillatory shear flow. As shown in Figure 1, periodic boundary conditions are used in the flow direction (x) and in the vorticity direction (z), whereas Lees–Edwards boundary conditions are used in the gradient direction (y).[48–52] Note that the simulation domain is chosen to be longer in the flow direction $L_x = 144 * Q_0$ than the width in the gradient and vorticity directions $L_w = 2.25Q_0$. This gives the particles sufficient time to diffuse across the width in the time they are advected in the flow direction, eliminating any bias created by using periodic boundary conditions in the flow direction. The time-dependent shear rate in the oscillatory flow is specified as

$$\dot{\gamma}(t) = \dot{\gamma}_0 \cos(\omega t), \tag{8}$$

where $\dot{\gamma}_0$ is the peak shear rate and ω is the frequency of oscillation. The shear strain is the integral of the shear rate and is sinusoidal with peak strain $\gamma = \dot{\gamma}_0/\omega$. The imposed velocity field is $v_x = \dot{\gamma}(t)y$, where x is the direction of flow along the length of the simulation box and y is the direction of velocity gradient. The dimensionless number which compares the imposed flow time scale ω^{-1} with the fluid relaxation time is the Deborah number De. Here, it is defined as

$$\mathrm{De} = \omega\lambda_\theta, \tag{9}$$

where $\lambda_\theta \simeq 1.7\zeta R_H^2/(k_B T)$ is the polymer relaxation time in theta solvent conditions for the 10 bead chain used here. The Deborah number quantifies whether the system has time to relax during the oscillations. The Weissenberg number is used to quantify the peak shear rate as $\mathrm{Wi} = \dot{\gamma}_0\lambda_\theta$. The ratio of the Weissenberg number to the Deborah number equals the peak strain amplitude.

To understand the response of the system, we will quantify the "state" of the system based on whether the polymer is stretched in an extended configuration or in a compact globule structure. The globule state is defined as the state in which the radius of gyration of the polymer R_g satisfies $R_g < 0.37R_{g,\theta}$ where $R_{g,\theta}$ is the equilibrium radius of gyration in theta conditions. The probability of this occurring at equilibrium without the colloids present is very small. For each condition of Wi and De, two simulations are performed, one in which the initial configuration is in the globule state and another in the stretched state. In most cases, the system looses memory of this starting configuration and produces the same results for the two simulations. The system is integrated for a time greater than $200\lambda_\theta$, which is sufficient to reach an oscillatory steady state (alternance) and measure multiple flow oscillations.

Because of the oscillatory flow, the stress in the fluid also oscillates. The stress contribution due to the beads τ_b (in addition to the Newtonian suspending solvent) in the BD simulations can be calculated by a sum of all pairs of beads[53,54]

$$\tau_b = \frac{1}{2V}\sum_m \sum_n \langle \mathbf{F}_{mn}\mathbf{R}_{mn}\rangle, \tag{10}$$

where m, n are the bead indices, $\mathbf{R}_{mn}$ is the vector connecting the bead pair, and $\mathbf{F}_{mn}$ is the net nonhydrodynamic forces acting between the pair. Once the system reaches alternance, the stress in the simulation can be averaged over multiple points in time provided the points are at the same point within a cycle. In this way, we obtain an averaged stress curve.

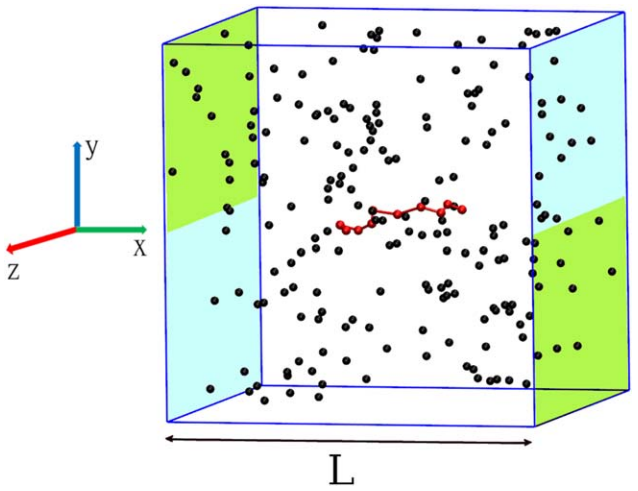

Figure 1. Snapshot of the simulation domain in which a single polymer molecule is surrounded by a sea of colloids.

[Color figure can be viewed in the online issue, which is available at wileyonlinelibrary.com.]

Discussion and Results

One method for analyzing the response of materials in LAOS is using a Lissajous curve, which is a plot of normalized shear stress vs. normalized strain.[55] For small strains, these curves are ellipses that look like a circle for a viscous material and look like a line for an elastic material. At large strains and large De, the curves deviate from ellipses. Because the Lissajous curves depend on Wi and De, we can draw Lissajous curve at each point in a Wi vs. De plot. To illustrate the prototypical features of such a plot, Figure 2 shows the Lissajous curves for a polymer model composed of a single FENE spring. For small Wi and small De (inside the dotted lines), the material approaches a Newtonian fluid and the curves become circles. For small strains (below the dot-dashed line), the response approaches the linear viscoelastic fluid and the curves are ellipses. For large strain and large Wi, the response is nonlinear.

For the model considered here of a mixture of a polymer and small colloids, the expected response is different, as shown in a sketch in Figure 3. At small enough De, the flow is pseudosteady; as the shear rate oscillates the material has time to respond to that condition as if it were steady shear. If $\mathrm{Wi} < \mathrm{Wi}_c$, the shear rate is never high enough to produce the stretched state, and the system remains as globules. If $\mathrm{Wi} > \mathrm{Wi}_c$, the polymer will stretch during the cycles (provided the strain is high enough). At large enough De, the peak strain drops below the value necessary to stretch the polymer and the system stays in the globule state. Our goal is to understand this regime at high Wi and high De and how the response changes from a viscous, pseudosteady behavior to the small strain linear viscoelastic response. By changing the strength of attractions of the polymer segments and the colloids, we can change the preference for the

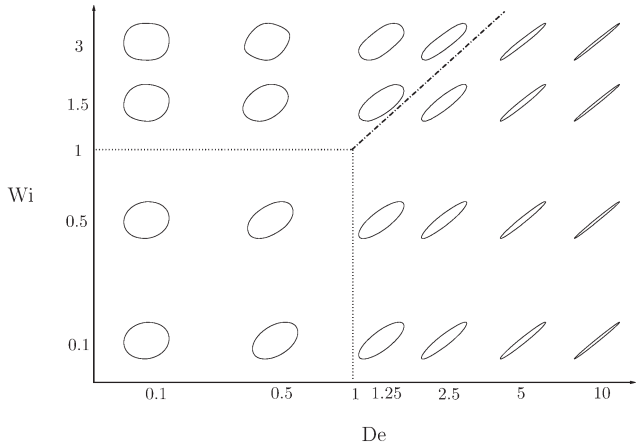

Figure 2. Sketch of Lissajous curves of normalized stress vs. strain for a polymer model composed of a single FENE spring at different Wi and De.

The dashed-dotted line is a strain of 1. The dotted lines are shown as a guide to the eye.

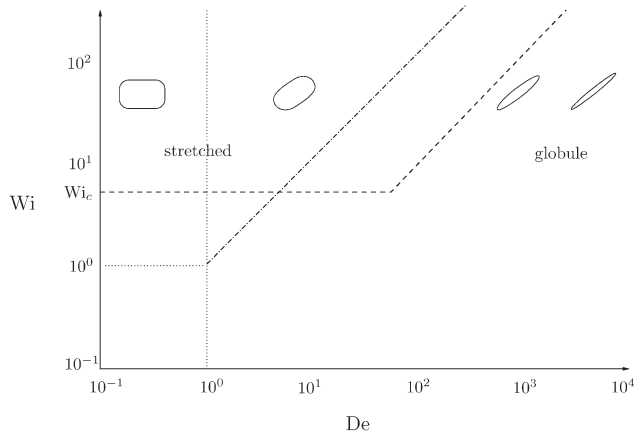

Figure 3. Sketch of the Wi vs. De space for a two state system that undergoes a globule-stretch transition including the Lissajous curves along constant Wi.

The dashed-dotted line represents a strain of 1 and the dotted lines are guides for the eye. The dashed line shows the boundary below which the dominant state is globules where Wi_c is the critical Wi for the globule-stretch in steady shear flow.

globule state. For the attractions examined here, the value of Wi_c is between 1 and 10. (Radhakrishnan and Underhill, under review)

Figure 4 shows the Lissajous curves for the largest strength of attractions $A^*=3.5$ at $Wi = 170$ and $Wi = 85$ for a range of De. The curves are compared to simulations with $A^*=0$, which corresponds to no electrostatic interactions. Within the statistical error bars of calculating the shear stress, the simulations starting from a globule and stretched state give the same response. Associated with each curve is the quantity g which is the fraction of the time of the simulation in which the polymer is in the globule state. Even at the relative large Wi, at the low end of the De range, the system spends a significant amount of time outside of the globule state. There is also qualitatively agreement between the interacting and noninteracting cases, suggesting that the polymer–colloid interactions are not controlling in the response. However, at higher De, the polymer-colloid attractions play an important role; more globules are formed and the response becomes more viscous. This is in sharp contrast to the noninteraction case (polymer only) which becomes almost purely elastic at high De. Because these higher De responses are close to ellipses, we can use the phase lag δ to quantify the shape and how viscous vs. elastic the response is. To do this, the Fourier transform is taken of the stress, and the storage modulus G' and loss modulus G'' are identified. The phase lag is defined as $\delta=\arctan(G''/G')$. Figure 5 shows the phase lag quantified from the data in Figure 4.

As mentioned previously, at lower De, the systems with and without interactions show similarly shaped Lissajous curves, and therefore similar phase lags. As De increases, the phase lag decreases and the system is more elastic; the frequency is high enough that the polymer does not have time to relax. However, the system with interactions shows the opposite trend; the system becomes more viscous and the phase lag increases as De increases. At higher De, the peak

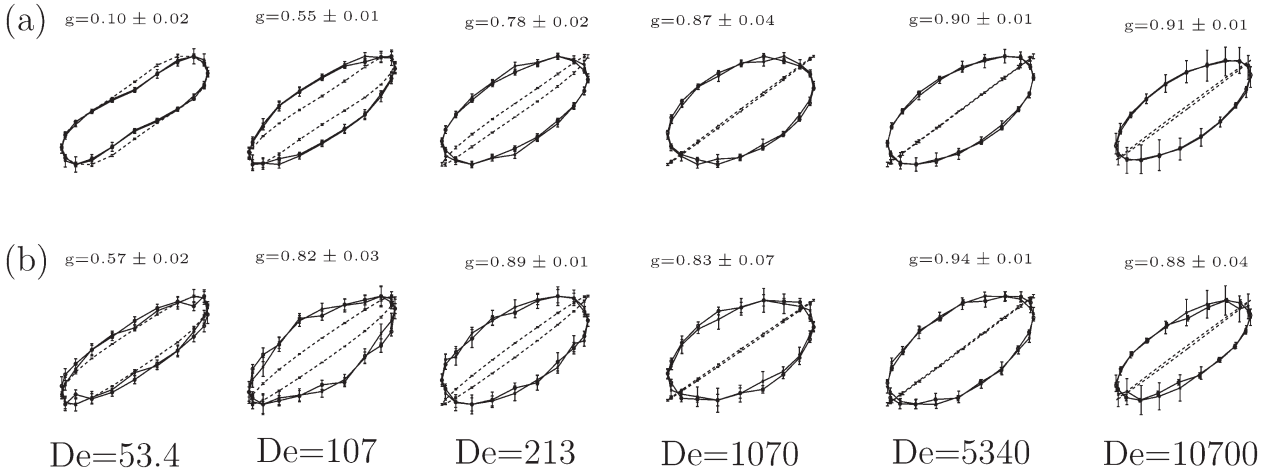

Figure 4. Lissajous curves of normalized stress vs. strain from BD simulations of polymer-colloid system at Wi = 170 (a) and Wi = 85 (b) for various values of De.

The Lissajous curves for $A^*=0$ (dashed) and $A^*=3.5$ (solid) are shown. The two solid curves representing different initial configurations of the polymer give the same results. The parameter g is the fraction of the time that the polymer is in the globule state.

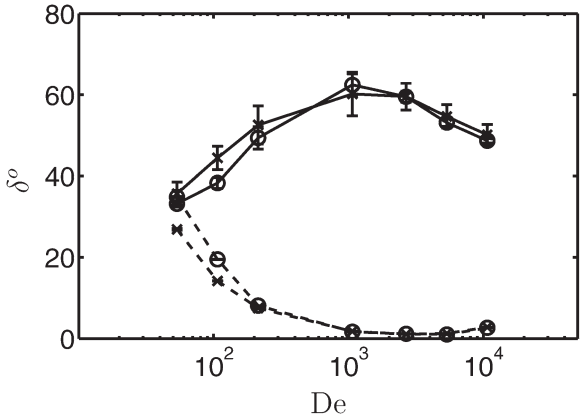

Figure 5. The phase lag δ in degrees between applied strain and shear stress is shown for a system with $A^*=0$ (dashed) and $A^*=3.5$ (solid) for Wi = 170 (○) and Wi = 85 (×) at different De.

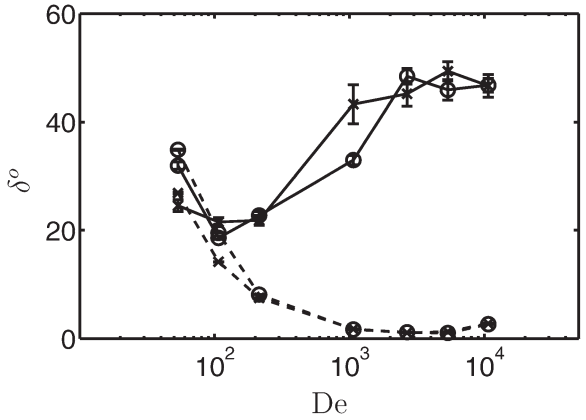

Figure 7. The phase lag δ in degrees between applied strain and shear stress is shown for a system with $A^*=0$ (dashed) and $A^*=3$ (solid) for Wi = 170 (○) and Wi = 85 (×) at different De.

strain is less leading to more globules. These globules can relax faster than the stretched polymer and hence give more of a viscous response. Eventually, the frequency (De) becomes high enough that even the globules cannot relax and the response starts becoming more elastic, corresponding to a drop in the phase lag.

We next use the same analysis method to examine a system with weaker attractions between the polymer segments and colloid beads, with $A^*=3$. Figures 6 and 7 show the Lissajous curves and extracted phase lags for this slightly weaker attraction. For this level of attraction, the time needed to form a globule is longer. At the lower values of De shown, the strain is large enough for the globules to stretch. However, when the shear rate drops below the critical globule-stretch value, the system does not have time to form a globule before the next cycle. Therefore, the system spends very little time the globule state and the response is very similar to the no-interaction case. As the frequency (De) is increased, the first effect is that the stretched polymers cannot relax, and the phase lag drops. At even higher De, the peak strain drops to the point that the globules cannot break, which leads to more globules (larger g). These globules have a faster relaxation time, and hence the response becomes more viscous with increasing De.

Figures 8 and 9 show the final step in the progression of even weaker interactions, with $A^*=2.5$. At this strength of interaction, the timescale for a globule to form is even further reduced, whereas at the same time making the globule that do form easier to pull apart. Because of these two properties, there are even fewer globules that form which leads to a close correspondence between the simulations with and without interactions. At very high De, the globules that formed are not able to be stretched by the flow because of the small peak strain, and the phase lag begins to increase.

Conclusions

In this article, we have used BD to perform computer simulations of a coarse-grained model of a dilute mixture of a polymer with nanoparticles in which they have short-ranged attractive interactions. The attractions can induce a collapse of the polymer into a compact globule state similar to a polymer in a poor solvent. In a shear flow, the globule can undergo a globule-stretch transition above a critical shear rate. Here, we have performed simulations in oscillatory shear flow in which the peak shear rate is above the globule-stretch transition. Because the flow oscillates, the shear rate

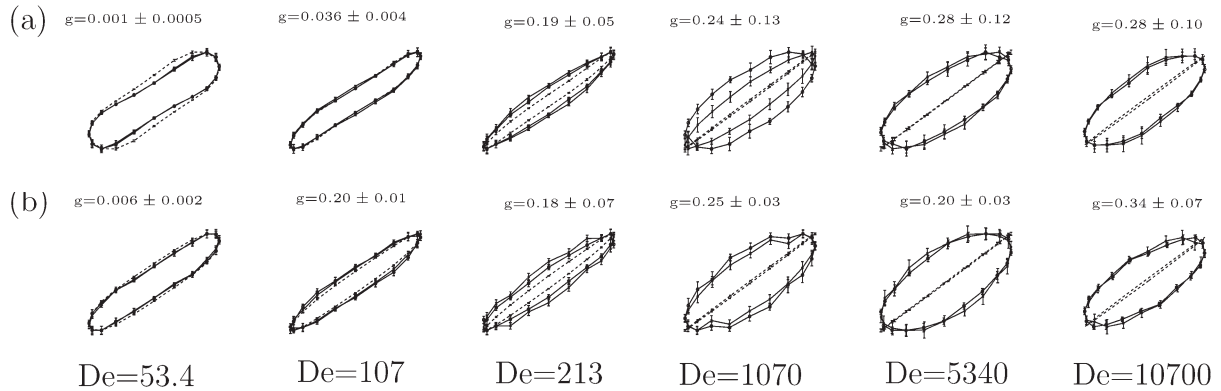

Figure 6. Lissajous curves of normalized stress vs. strain from BD simulations of polymer-colloid system at Wi = 170 (a) and Wi = 85 (b) for various values of De.

The Lissajous curves for $A^*=0$ (dashed) and $A^*=3$ (solid) are shown. The two solid curves representing different initial configurations of the polymer give the same results for most cases. The parameter g is the fraction of the time that the polymer is in the globule state.

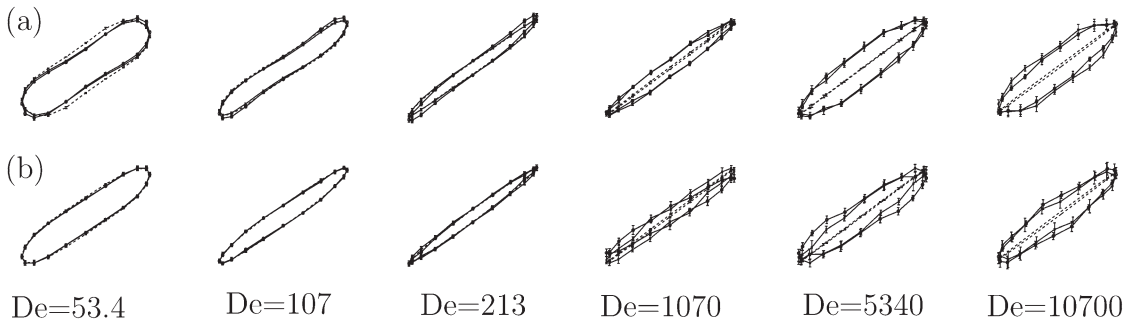

Figure 8. Lissajous curves of normalized stress vs. strain from BD simulations of polymer-colloid system at Wi = 170 (a) and Wi = 85 (b) for various values of De.

The Lissajous curves for $A^*=0$ (dashed) and $A^*=2.5$ (solid) are shown. The two solid curves representing different initial configurations of the polymer give the same results.

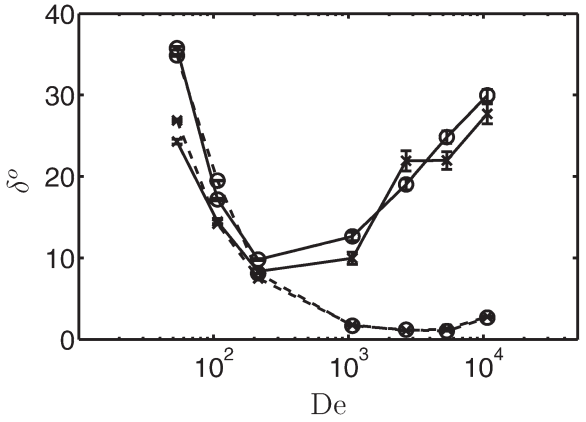

Figure 9. The phase lag δ in degrees between applied strain and shear stress is shown for a system with $A^*=0$ (dashed) and $A^*=2.5$ (solid) for Wi = 170 (○) and Wi = 85 (×) at different De.

will also reach very small values and globules will still exist. In fact, if the frequency of oscillation is high enough, the small strain does not allow the globule to stretch out.

These transitions between states that are caused by the flow also impact the rheological properties. We have shown that the change of the Lissajous curves with Wi and De can see these transitions. In particular, in the linear region, the phase lag can quantify the viscous vs. elastic response. At small enough De that the system is primarily in the stretched state, the response becomes more elastic as De increases. Eventually, the increasing frequency leads to a transition to the globule state which has a smaller relaxation time, and therefore a more viscous response. We expect this type of response to be common among systems which can exist in multiple states and in which flow can induce changes between those states. Therefore, nonmontonic changes in the viscous vs. elastic character of a fluid could serve as an experimental signature of such systems. We are not aware of any previous experimental studies that show this nonmonotonic change and believe polymers in poor solvents or mixtures of polymers and nanoparticles could be such a system.

Acknowledgment

We gratefully acknowledge support by NSF Grant No. CBET-0954445.

Literature Cited

1. Srivastava S, Shin JH, Archer LA. Structure and rheology of nanoparticle–polymer suspensions. *Soft Matter*. 2012;8:4097–4108.
2. Wang J, Bai R, Joseph DD. Nanoparticle-laden tubeless and open siphons. *J Fluid Mech*. 2004;516:335–348.
3. Balazs AC, Emrick T, Russell TP. Nanoparticle polymer composites: where two small worlds meet. *Science*. 2006;314:1107–1110.
4. Zhang G, Wu C. Reentrant coil-to-globule-to-coil transition of a single linear homopolymer chain in a water /methanol mixture. *Phys Rev Lett*. 2001;86:822–825.
5. Hyeon C, Morrison G, Pincus DL, Thirumalai D. Refolding dynamics of stretched biopolymers upon force quench. *Proc Natl Acad Sci USA*. 2009;106:20288–20293.
6. Lee N, Thirumalai D. Dynamics of collapse of flexible polyampholytes. *J Chem Phys*. 2000;113:5126–5129.
7. Kiriy A, Gorodyska G, Minko S, Jaeger W, Stepanek P, Stamm M. Cascade of coil-globule conformational transitions of single flexible polyelectrolyte molecules in poor solvent. *J Am Chem Soc*. 2002; 124:13454–13462.
8. Dobrynin AV, Rubinstein M. Theory of polyelectrolytes in solutions and at surfaces. *Prog Polym Sci*. 2005;30:1049–1118.
9. Zinchenko AA, Yoshikawa K, Baigl D. Compaction of single-chain DNA by histone-inspired nanoparticles. *Phys Rev Lett*. 2005;95: 228101.
10. Estevez-Torres A, Baigl D. DNA compaction: fundamentals and applications. *Soft Matter*. 2011;7:6746–6756.
11. Zhou K, Lu Y, Li J, Shen L, Zhang G, Xie Z, Wu C. The coil-to-globule-to-coil transition of linear polymer chains in dilute aqueous solutions: effect of intrachain hydrogen bonding. *Macromolecules*. 2008;41:8927–8931.
12. Murnen HK, Khokhlov AR, Khalatur PG, Segalman RA, Zuckermann RN. Impact of hydrophobic sequence patterning on the coil-to-globule transition of protein-like polymers. *Macromolecules*. 2012;45:5229–5236.
13. Otsubo Y. Dilatant flow of flocculated suspensions. *Langmuir*. 1992; 8:2336–2340.
14. Kamibayashi M, Ogura H, Otsubo Y. Shear-thickening flow of nanoparticle suspensions flocculated by polymer bridging. *J Colloid Interface Sci*. 2008;321:294–301.
15. Jonsson M, Linse P. Polyelectrolyte–macroion complexation. I. Effect of linear charge density, chain length, and macroion charge. *J Chem Phys*. 2001;115:3406–3418.
16. Shen AQ, Gleason B, McKinley GH, Stone HA. Fiber coating with surfactant solutions. *Phys Fluids*. 2002;14:4055–4068.
17. Hansson P, Lindman B. Surfactant-polymer interactions. *Curr Opin Colloid Interface Sci*. 1996;1:604–613.
18. Thastrom A, Lowary PT, Widom J. Measurement of histone–DNA interaction free energy in nucleosomes. *Methods*. 2004;33:33–44.
19. Krotova MK, Vasilevskaya VV, Makita N, Yoshikawa K, Khokhlov AR. DNA compaction in a crowded environment with negatively charged proteins. *Phys Rev Lett*. 2010;105:128302.
20. Yoshikawa K, Hirota S, Makita N, Yoshikawa Y. Compaction of DNA induced by like-charge protein: opposite salt-effect against the polymer-salt-induced condensation with neutral polymer. *J Phys Chem Lett*. 2010;1:1763–1766.

21. Nandy B, Maiti PK. DNA compaction by a dendrimer. *J Phys Chem B*. 2011;115:217–230.
22. Liu H, Wang H, Yang W, Cheng Y. Disulfide cross-linked low generation dendrimers with high gene transfection efficacy, low cytotoxicity, and low cost. *J Am Chem Soc*. 2012;134:17680–17687.
23. Kabanov AV, Kabanov VA. DNA complexes with polycations for the delivery of genetic material into cells. *Bioconjug Chem*. 1995;6: 7–20.
24. Alexander-Katz A, Schneider MF, Schneider SW, Wixforth A, Netz RR. Shear-flow-induced unfolding of polymeric globules. *Phys Rev Lett*. 2006;97:138101.
25. Schneider SW, Nuschele S, Wixforth A, Gorzelanny C, Alexander-Katz A, Netz RR, Schneider MF. Shear-induced unfolding triggers adhesion of von willebrand factor fibers. *Proc Natl Acad Sci USA*. 2007;104:7899–7903.
26. Sing CE, Alexander-Katz A. Globule–stretch transitions of collapsed polymers in elongational flow fields. *Macromolecules*. 2010;43: 3532–3541.
27. Sing CE, Alexander-Katz A. Giant nonmonotonic stretching response of a self-associating polymer in shear flow. *Phys Rev Lett*. 2011;107: 198302.
28. Hoda N, Larson RG. Brownian dynamics simulations of single polymer chains with and without self-entanglements in theta and good solvents under imposed flow fields. *J Rheol*. 2010;54:1061–1081.
29. Hyun K, Wilhelm M, Klein CO, Cho KS, Nam JG, Ahn KH, Lee SJ, Ewoldt RH, McKinley GH. A review of nonlinear oscillatory shear tests: analysis and application of large amplitude oscillatory shear (LAOS). *Prog Polym Sci*. 2011;36:1697–1753.
30. Ewoldt RH, Hosoi AE, McKinley GH. Rheological fingerprinting of complex fluids using large amplitude oscillatory shear (LAOS) flow. *Annu Trans Nordic Rheol Soc*. 2007;15:3.
31. de Gennes PG. Coil-stretch transition of dilute flexible polymers under ultrahigh velocity gradients. *J Chem Phys*. 1974;60:5030–5042.
32. Hinch EJ. Mechanical models of dilute polymer solutions in strong flows. *Phys Fluids*. 1977;20:S22–S30.
33. Schroeder CM, Babcock HP, Shaqfeh ESG, Chu S. Observation of polymer conformation hysteresis in extensional flow. *Science*. 2003; 301:1515–1519.
34. Warner HR. Kinetic theory and rheology of dilute suspensions of finitely extendible dumbbells. *Ind Eng Chem Res*. 1972;11:379–387.
35. Weeks JD, Chandler D, Andersen HC. Role of repulsive forces in determining the equilibrium structure of simple liquids. *J Chem Phys*. 1971;54:5237–5247.
36. Ermak DL, McCammon JA. Brownian dynamics with hydrodynamic interactions. *J Chem Phys*. 1978;69:1352–1361.
37. Beard DA, Schlick T. Computational modeling predicts the structure and dynamics of chromatin fiber. *Structure*. 2001;9:105–114.
38. Grassia PS, Hinch EJ, Nitsche LC. Computer simulations of Brownian motion of complex systems. *J Fluid Mech*. 1995;282:373–403.
39. Cifre JGH, de la Torre JG. Steady-state behavior of dilute polymers in elongational flow. Dependence of the critical elongational rate on chain length, hydrodynamic interaction, and excluded volume. *J Rheol*. 1999;43:339–358.
40. Underhill PT, Doyle PS. On the coarse-graining of polymers into bead-spring chains. *J Non-Newtonian Fluid Mech*. 2004;122:3–31.
41. Jendrejack RM, de Pablo JJ, Graham MD. Stochastic simulations of DNA in flow: dynamics and the effects of hydrodynamic interactions. *J Chem Phys*. 2002;116:7752–7760.
42. Larson RG. The rheology of dilute solutions of flexible polymers: progress and problems. *J Rheol*. 2005;49:1–70.
43. Shaqfeh ESG. The dynamics of single-molecule DNA in flow. *J Non-Newtonian Fluid Mech*. 2005;130:1–28.
44. Schroeder CM, Teixeira RE, Shaqfeh ESG, Chu S. Dynamics of DNA in the flow-gradient plane of steady shear flow: observations and simulations. *Macromolecules*. 2005;38:1967–1978.
45. Hur JS, Shaqfeh ESG, Babcock HP, Smith DE, Chu S. Dynamics of dilute and semidilute DNA solutions in the start-up of shear flow. *J Rheol*. 2001;45:421–451.
46. Babcock HP, Smith DE, Hur JS, Shaqfeh ESG, Chu S. Relating the microscopic and macroscopic response of a polymeric fluid in a shearing flow. *Phys Rev Lett*. 2000;85:2018–2021.
47. Prakash JR. Rouse chains with excluded volume interactions: linear viscoelasticity. *Macromolecules*. 2001;34:3396–3411.
48. Lees AW, Edwards SF. The computer study of transport processes under extreme conditions. *J Phys C Solid State*. 1972;5:1921–1929.
49. Jose PP, Szamel G. Single-chain dynamics in a semidilute polymer solution under steady shear. *J Chem Phys*. 2008;128:224910.
50. Jose PP, Szamel G. Structure of a semidilute polymer solution under steady shear. *J Chem Phys*. 2007;127:114905.
51. Stoltz C, de Pablo JJ, Graham MD. Simulation of nonlinear shear rheology of dilute salt-free polyelectrolyte solutions. *J Chem Phys*. 2007;126:124906.
52. Fetsko SW, Cummings PT. Simulation of bead-and-spring chain models for semidilute polymer solutions in shear flow. *Int J Thermophys*. 1994;15:1085–1091.
53. Doi M, Edwards SF. *The Theory of Polymer Dynamics*. New York: Oxford University Press, 1988.
54. Bird RB, Armstrong RC, Hassager O, Curtiss CF. *Dynamics of Polymeric Liquids*, Vol. 2. New York: Wiley, 1987.
55. Philippoff W. Vibrational measurements with large amplitudes. *Trans Soc Rheol*. 1966;10:317–334.

Manuscript received Oct. 11, 2013, and revision received Jan. 5, 2014.